Journal of the European Ceramic Society 22 (2002) 1723–1728

www.elsevier.com/locate/jeurceramsoc

Physical characteristics and sintering behavior of ultrafine zirconia–ceria powders

S.K. Tadokoro, E.N.S. Muccillo*

Multidisciplinary Center for Development of Ceramic Materials, CCTM- Energy and Nuclear Research Institute, C.P. 11049, Pinheiros, Sao Paulo, SP 05422-970, Brazil

Received 27 March 2001; received in revised form 21 September 2001; accepted 7 October 2001

Abstract

Ultrafine zirconia–12 mol% ceria powders have been prepared by the coprecipitation technique. The azeotropic distillation with *n*-butanol has been carried out to ensure complete elimination of the residual water in the precipitate. This procedure has proved to be quite effective in preventing the formation of agglomerates, which are responsible for inhomogeneities in the sintered microstructure, and for non-densification at low temperatures. The crystallization of the solid solution occurs at 430 °C as determined by thermal analyses. The specific surface of the calcined powder is 127.9 $m^2 g^{-1}$ and the pore size distribution exhibits only a maximum at approximately 9 nm. Total shrinkage of the compacted powder reached 30% at 1200 °C. Sintered specimens show six bands characteristics of the tetragonal phase in the Raman spectrum. Specimens with apparent densities >95% of the theoretical density and average grain size of 230–400 nm were obtained after sintering at 1200 °C.

Keywords: TZP; Powders–chemical preparation; Sintering; ZrO_2-CeO_2

1. Introduction

Zirconia-based solid solutions are one of the most studied solid oxide electrolyte systems due to many practical applications of these ceramics. Tetragonal zirconia polycrystals doped either with yttrium (Y–TZP) or cerium (Ce–TZP) have received great attention because of their optimal thermomechanical properties. Ce-TZP ceramics have high fracture toughness and high thermal stability compared to Y–TZP ceramics.[1]

Earlier studies on zirconia-ceria solid solution have shown that sintering temperatures might be relatively high, in order to attain a high densification. However, at these high temperatures (⩾1200 °C) some loss of oxygen due to Ce^{4+} reduction to Ce^{3+} was observed.[2,3] In addition, the grain sizes of sintered ceramics are, in general, between 1 μm and 4 μm. It was shown further that the rate of grain growth in Ce-TZP is faster than that in Y-TZP ceramics.[4] Some studies[5,6] have revealed that minor additions of divalent or trivalent cations are quite effective to suppress the grain boundary mobility and, consequently, grain growth. Moreover, these impurities have reduced the average grain sizes to a minimum of about 1 μm. It is well known that there is a strong correlation between grain size and mechanical properties. The fracture toughness increases with increasing grain size whereas the Vickers hardness shows the opposite trend. The bending strength of specimens with different grain sizes is higher for specimens having smaller grain sizes.[7]

The properties of ceramic materials strongly depend on their chemical, physical and structural characteristics, which are determined by the preparation methods. Several efforts have been performed in recent years to improve the sinterability and final microstructure of Ce–TZP ceramics. Solid solutions in this system have been prepared by a variety of methods like mixing of oxides,[8] coprecipitation,[2,9–14] mechanical alloying,[13] sol-gel[15,16] and rapid solidification.[17] The mechanical alloying of this solid solution has resulted in ceramics with an average grain size of 0.5 μm and 92% of relative density after sintering at 1450 °C/3 h.[13] Recently an improvement on grain size (∼ 0.5 μm) and densification

* Corresponding author.
E-mail addresses: enavarro@usp.br (E.N.S. Muccillo) sktadok@net.ipen.br (S.K. Tadokoro).

0955-2219/02/$ - see front matter
PII: S0955-2219(01)00475-7

(>98% of the theoretical density) has been achieved simply by means of a suitable choice of parameters involved in the coprecipitation process.[14]

Concerning powder preparation by the coprecipitation technique, it was recently shown that improved powder characteristics could be obtained by using the azeotropic distillation in the dehydration step[18, 19]. This technique has proved to be quite efficient to eliminate the residual water in the precipitate responsible for the formation of hard agglomerates. For Y–TZP, for example, nanosized powders in the 10–20 nm range and specific surface of 53.5 $m^2\ g^{-1}$ was prepared. This powder resulted in sintered ceramics with 200–300 nm grain sizes.[18] For the composite ZrO_2–Al_2O_3, a nanosized powder (~20 nm) resulted in an average grain size of 0.2 μm after sintering at 1300 °C.[19]

In this work, the azeotropic distillation was used to obtain highly sinterable nanosized powders of zirconia-12 mol% ceria. The main purpose of this work is to optimize the preparation methods in order to attain high densification along with a reduced grain size.

2. Experimental procedure

2.1. Powder and specimens preparations

ZrO_2. n H_2O (>99%) and cerium nitrate (>99%) both produced at this Institute were used as starting materials. All other reagents were of analytical grade. Zirconyl chloride crystals were prepared by dissolution of the hydrated zirconium oxide in a hot 6M HCl solution. After some time under constant evaporation, crystals of zirconyl chloride started to growth. These crystals were washed in acetone and dried inside a dessicator. Aqueous solutions of both precursors were separately prepared. Suitable amounts of these solutions were mixed together under stirring in order to obtain a homogeneous 0.1M cation solution. This solution was dropped at a rate of 50 ml min^{-1} over a 5M NH_4OH solution to effect the precipitation in a pH >9. The precipitate was washed with ammonia (10 vol.%) solution until most of Cl^- ions were eliminated. The washing with diluted ammonia greatly improves the chloride elimination due to the formation of NH_4Cl. Moreover, after some washing cycles with the ammonia solution a test with 1M $AgNO_3$ solution is usually performed. Dehydration was carried out with absolute ethanol and isopropyl alcohol washings. Then, the precipitate was dispersed in *n*-butyl alcohol and distilled. For the azeotropic distillation step a simple set up was used.[19] After distillation, the dispersion was vacuum filtered and the gel was dried in an oven at 45 °C and gently deagglomerated in an agate mortar. The nominal concentration of CeO_2 in the solid solution was 12 mol%.

2.2. Characterizations

Thermal decomposition of the gel was monitored by thermogravimetric, TG, and differential thermal analyses, DTA (STA 409, Netzsch), heating at a rate of 10 °C min^{-1} up to 1000 °C in air. Alpha alumina was used as reference material in DTA runs. The distribution of particle sizes in the calcined powder was obtained by laser scattering (Granulometer 1064, Cilas). Nitrogen adsorption/desorption (ASAP 2010, Micromeritics) experiments have been carried out to determine the specific surface area, S, by the Brunauer, Emmett and Teller (BET) method and the distribution of pore sizes by the Barret, Joyner and Halenda (BJH) method. X-ray diffraction patterns of calcined powders were obtained in a diffractometer (D8 Advance, Bruker-AXS) using Cu K_α radiation at 40 kV and 40 mA in the 20–90° 2θ range and a step size of 0.05° 3 s^{-1}.

Cylindrical specimens were obtained by uniaxial followed by isostatic pressing at 206 MPa. Linear shrinkage (DIL 402 ES, Netzsch) in the powder compact was followed up to 1600 °C with a heating rate of 10 °C. min^{-1}.

Sintering experiments were performed in air in a tubular furnace with a heating rate of 10 °C min^{-1}. The apparent density values of sintered ceramics were measured by the water displacement method. Particle morphology in the calcined powder, and grain size and shape in sintered ceramics were observed by scanning electron microscopy, SEM (LEO 440I, Oxford). The average grain sizes in compacts sintered at different times were calculated by a homemade program based on the Saltikov statistical analysis. Phase determination was performed by Raman spectroscopy (Renishaw Raman Microscope System 3000 coupled to an Olympus BH-2 microscope and to a CCD detector cooled by Peltier). An exciting radiation of 514.5 nm from an Ar^+ laser (Omnichrome, model 170) was used.

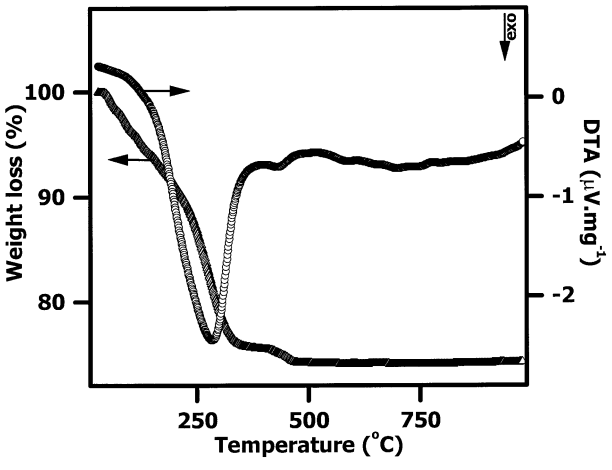

Fig. 1. TG and DTA curves of the zirconia–ceria dried gel.

3. Results and discussion

3.1. Powder materials

TG and DTA curves of the dried gel are shown in Fig. 1. The weight loss is substantial up to 400 °C and is negligible beyond this temperature. Total weight loss is about 27%. It was proposed earlier[20] that when coprecipitating Zr^{4+} and Ce^{3+} cations, cerium enters into solid solution in a trivalent state. However, it is generally known that when cerium hydroxide is precipitated, it slowly oxidizes in contact with air.[21] The continuous changes observed in the color of the precipitate during subsequent processing just after precipitation, suggests that both Ce^{4+} and Ce^{3+} may be present in the precipitated hydroxides. The weight loss observed is attributed to the thermal decomposition of the precipitated hydroxides and to the residual organic matter from alcohol washings.

The DTA curve shows two exothermic peaks centered at 280 and 430 °C. Most of previous results on thermal analyses of zirconia-ceria prepared by the coprecipitation technique exhibit a low-temperature endothermic peak.[10,22] This endothermic peak is attributed to loss of water. In the present work, no endothermic peak is detected because of the high efficiency of the azeotropic distillation for water removal, and the alcohol evolution. The peak at 280 °C can be assigned to alcohol combustion. The exothermic peak at 430 °C is due to the crystallization of the solid solution in agreement with a previous observation.[10] According to these results, a temperature of 450 °C was chosen for calcination of the gel. Such a low temperature for calcination seems to be convenient, in this case, because it has already been observed that the crystallite size may influence the grain size of the sintered ceramic.[13,14]

Fig. 2 shows the distribution of particle sizes after calcination of the precipitate at 450 °C/1 h. This curve may not truly represent the particle size distribution, as certain powder agglomerates might not be properly dispersed during the process of sample preparation for this characterization. However, this curve does indicate the average degree of powder agglomeration in the solid solution. The average particle/agglomerate size obtained at 50% cumulative mass is 23.4 μm.

A typical micrograph of the calcined powder obtained in a scanning electron microscope is shown in Fig. 3. As usually expected for fine powders, these particles are agglomerated with an enlarged distribution and without uniformity in size and shape.

Even though the results on laser scattering and scanning electron microscopy give information regarding the distribution and shape of particles/agglomerates, they are not sufficient for the evaluation of the strength of these agglomerates.

Fig. 4 shows the X-ray diffraction pattern of the calcined powder. The main observed feature is the presence of peaks of the tetragonal (ICDD 17-923) solid solution. The widths of the peaks are characteristic of a low-crystalline material as expected for such a low calcination temperature.

A typical adsorption/desorption isotherm is shown in Fig. 5. This isotherm is of type IV (BDDT classification),[23]

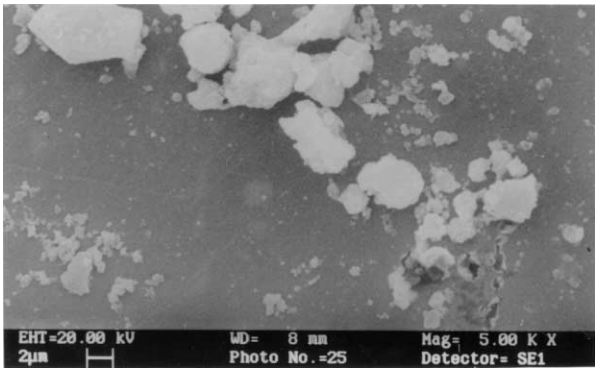

Fig. 3. SEM micrograph of zirconia–ceria calcined powder.

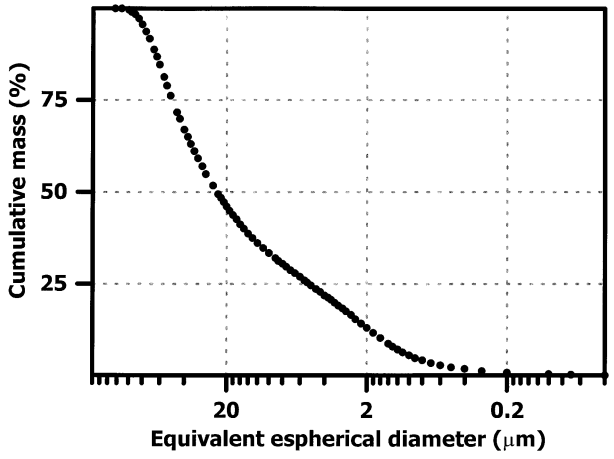

Fig. 2. Particle size distribution of zirconia–ceria calcined powder obtained by laser scattering.

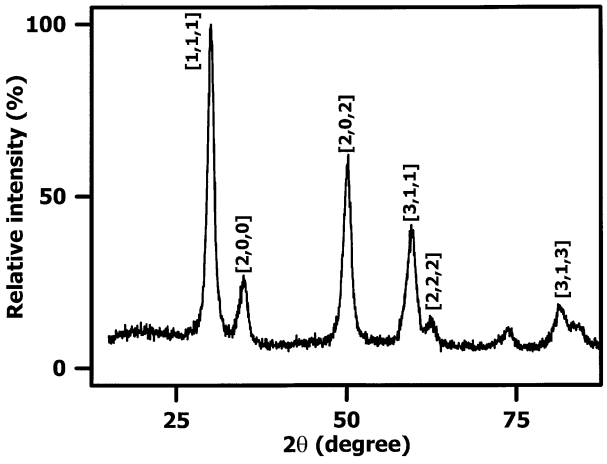

Fig. 4. X-ray diffraction pattern of zirconia–ceria calcined powder .

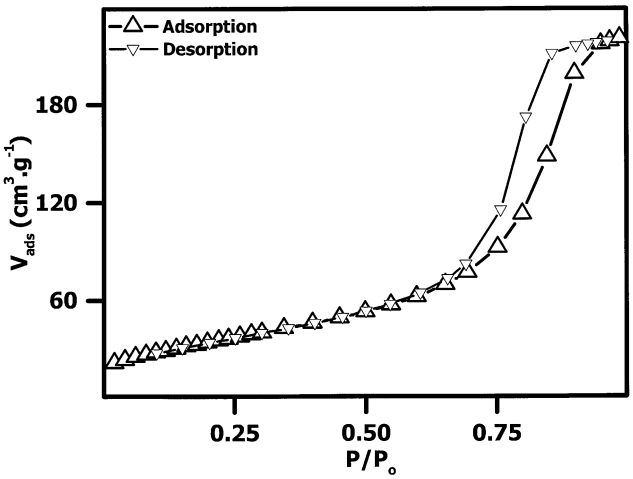

Fig. 5. Adsorption/desorption isotherm of zirconia–ceria calcined powder.

characteristic of a well-developed system containing mesopores (pores with diameters between 2.0 and 50.0 nm). The hysteresis loop is characterized by adsorption and desorption branches nearly parallel to each other in a considerable range of P/P_0. This type of loop is frequently obtained for approximately spherical agglomerated particles with uniform size and coordination number. The value of the specific surface area determined by the BET method is 127.9 $m^2\ g^{-1}$.

Fig. 6 shows the pore size distribution curve obtained by the BJH method, assuming a cylindrical pore model. The majority of the results obtained for zirconia-based solid solutions prepared by chemical techniques do not show a monomodal distribution, as shown here. Conventional zirconia usually presents a bimodal distribution of pore sizes, which corresponds to intra- and inter-agglomerate pores. The latter are removed later during sintering, taking part in the densification process and influencing grain growth rates.[24] Therefore, the distribution shown in Fig. 6 shows that the agglomerates responsible for the slowdown in the densification process have not been formed. The average pore size is 9 nm.

3.2. Compacted and sintered specimens

The linear shrinkage of a powder compact is shown in Fig. 7. Higher shrinkage occurs between 930 and 1200 °C. For temperatures higher than 1200 °C the grain growth mechanism predominates. Total shrinkage of the compact is about 30% and the temperature of maximum shrinkage is 1150 °C as determined by the derivative curve. It is already known that Ce–TZP densifies via liquid phase sintering and that Si and Ca impurities are essential to attain full densification.[1] Although these impurities may be detrimental to some properties in the sintered material, they are frequently found in starting materials.

Previous dilatometric experiments performed on specimens prepared by the same synthesis technique[12,13] exhibit a total shrinkage less than 17% at 1400 °C. These contrasting results can be attributed to the better powder properties reported here. It is known that agglomerates may be formed in powders prepared by chemical techniques. Moreover, it is generally accepted that these agglomerates can be classified, according to their mechanical strength, into soft (those that are easily broken during pressing), and hard (those that remain in the compacted powder). It was shown that the strength of agglomerates in powders prepared by a chemical route is determined by the extent to which water molecules, hydrogen-bonded to surface hydroxyl groups, are able to form bridges between adjacent particles.[25] The use of organic liquids greatly enhances the elimination of water from the precipitates. However, this procedure does not allow for complete elimination of residual water even when isopropyl alcohol, known as a scavenger for hydroxyl ions, is used. The distillation of the

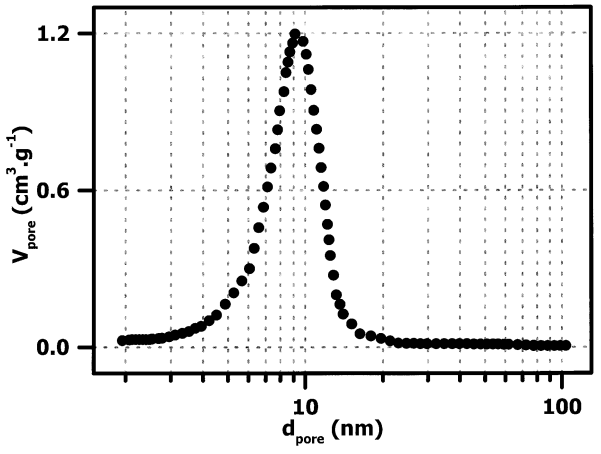

Fig. 6. Pore size distribution, obtained by the BJH method, of zirconia–ceria calcined powder.

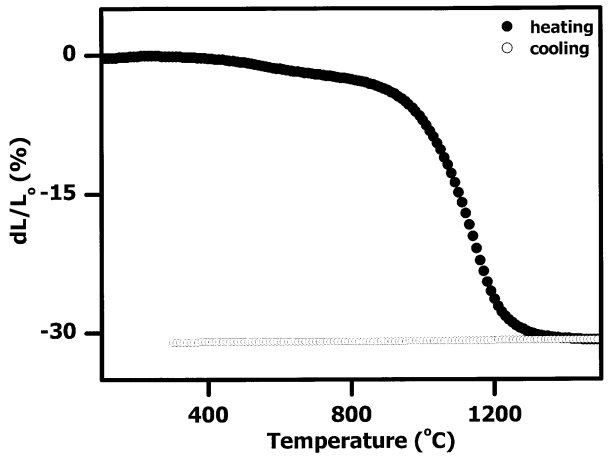

Fig. 7. Linear shrinkage curve of a zirconia–ceria powder compact.

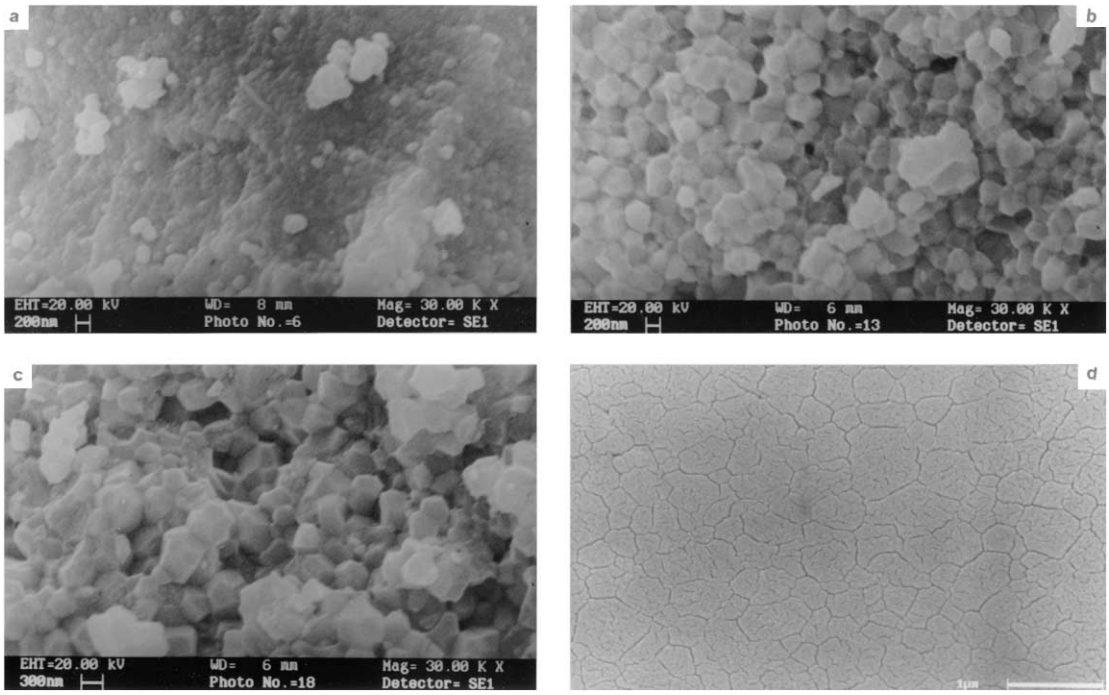

Fig. 8. SEM micrographs of fractured surfaces of zirconia–ceria specimens sintered at 1200 °C for 1 h (a), 5 h (b), and 8 h (c); a polished and thermally etched surface of a specimen sintered for 8 h is shown in (d).

Table 1
Apparent density values and average grain sizes as a function of soaking time at 1200 °C

Soaking time (h)	Sintered density (g cm^{-3})	Grain size (nm)
1	5.98	230
5	6.18	280
8	6.03	400

gel is quite important to reduce the water content to a level that it does not interfere with the development of the microstructure and physical properties of the sintered ceramic. The mechanism of the azeotropic distillation to prevent the formation of hard agglomerates was studied and thoroughly discussed elsewhere.[18]

From this result, a temperature of 1200 °C was chosen for sintering experiments with soaking times of 1 h, 5 h, and 8 h. Table 1 shows apparent density values obtained according to these sintering conditions.

The sintered density initially increases with soaking time up to 5 h reaching a relative density of 98%. A value of 6.29 g cm^{-3} was used as the theoretical density.[14] A further increase in the sintering time to 8 h produced a decrease in the density (96%). This decrease in the sintered density with prolonged soaking times is believed to be related with some loss of oxygen due to the reduction of Ce^{4+}–Ce^{3+}. Even though it has already been shown[3] that the reduction reaction starts at about 1200 °C, further experiments are necessary to be sure of this reduction process.

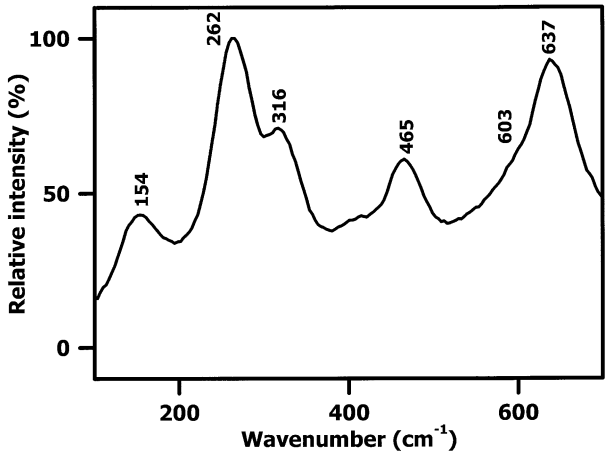

Fig. 9. Raman spectrum of a zirconia–ceria sintered specimen.

The effect of the sintering time at 1200 °C on the grain sizes is shown in Table 1 and in the micrographs of Fig. 8(a–c). As expected, there is a fast increase in grain size with the soaking time at this temperature. Fig. 8d shows a representative scanning electron microscopy micrograph of a polished and thermally etched surface obtained for the specimen sintered at 1200 °C for 8 h. The main microstructural features are a uniform grain size along with a low porosity.

Fig. 9 shows the Raman spectrum of a zirconia-ceria specimen sintered at 1200 °C/1 h. The six bands observed are characteristics of the tetragonal phase[26] in zirconia-based solid solutions, and no traces of the

active Raman modes corresponding to the monoclinic phase were detected.

4. Conclusions

Ultrafine zirconia-ceria powders have been prepared by the coprecipitation technique. The use of azeotropic distillation for gel dehydration greatly improves the physical properties of the solid solution. Powders with specific surface area larger than 120 $m^2\ g^{-1}$ and average pore size of 9 nm have been obtained. This powder allowed for preparing ceramic specimens with relative densities $>95\%$, average grain sizes <300 nm, and total stabilization of the tetragonal phase at a sintering temperature as low as 1200 °C.

Acknowledgements

To the Powder Processing Center at IPEN for the nitrogen adsorption measurements. To the Laboratory of Powder Metallurgy and Magnetic Materials of the Institute for Technological Research (IPT, Sao Paulo, Brazil) for dilatometric experiments. To FAPESP (94/05929-5, 95/05635-4, 95/05172-4, 96/09604-9 and 99/10798-0) that sponsored most of the facilities used in this work. To CNPq (300934/94-7). One of the authors (S.K.T.) acknowledges FAPESP (98/09976-9) for the scholarship.

References

1. Cawley, J. D. and Lee, W. E. Oxide ceramics. In *Materials Science and Technology, a Comprehensive Treatment*, ed. R. W. Cahn, P. Haasen, E. J. Kramer, vol. 11. *Structure and Properties of Ceramics*, ed. M. V. Swain, VCH, Weinheim, Germany, 1994, pp. 47–117.
2. Durán, P., Gonzalez, M., Jurado, J. R. and Moure, C., Processing–microstructurebtqmechanical properties relationship in Ce-doped tetragonal zirconia. In *Ceramic Powder Science III, Ceramic Transactions 12*, ed. G. L. Messing, S. I. Hirano and H. Hausner. Am. Ceram. Soc, Westerville, OH, 1990, pp. 945–952.
3. Theunissen, G. S. A. M., Winnubst, A. J. A. and Burggraaf, A. J., Effect of dopants on the sintering behaviour and stability of tetragonal zirconia ceramics. *J. Eur. Ceram. Soc.*, 1992, **9**, 251–263.
4. Sato, T. and Shimada, M., Transformation of ceria-doped tetragonal zirconia polycrystals by annealing in water. *Am. Ceram. Soc. Bull.*, 1985, **64**, 1382–1384.
5. Hwang, S.-L. and Chen, I.-W., Grain size control of tetragonal zirconia polycrystals using the space charge concept. *J. Am. Ceram. Soc.*, 1990, **73**, 3269–3277.
6. Park, J.-H. and Moon, S.-W., Stability and sinterability of tetragonal zirconia polycrystals costabilized by CeO_2 and various oxides. *J. Mater Sci. Lett.*, 1992, **11**, 1046–1048.
7. Tsukuma, K. and Shimada, M., Strength, fracture toughness and Vickers hardness of CeO_2-stabilized tetragonal ZrO_2 polycrystals (Ce–TZP). *J. Mater Sci.*, 1985, **20**, 1178–1184.
8. Wang, J. S., Tsai, J. F., Shetty, D. K. and Virkar, A. V., Effect of MnO on the microstructures, phase stability, and mechanical properties of ceria partially-stabilized zirconia (Ce–TZP) and Ce–TZP-Al_2O_3 composites. *J. Mater. Res.*, 1990, **5**, 1948–1957.
9. Duh, J.-G., Dai, H.-T. and Hsu, W. Y., Synthesis and sintering behaviour in CeO_2–ZrO_2 ceramics. *J. Mater Sci.*, 1988, **23**, 2786–2791.
10. Sato, T., Dosaka, K., Yoshioka, T., Okuwaka, A., Yorii, K. and Onodera, Y., Sintering of ceria-doped tetragonal zirconia crystallized in organic solvents, water, and air. *J. Am. Ceram. Soc.*, 1992, **75**, 552–556.
11. Houte, S. El, Stable/metastable Ce–TZP, effect of chemical composition and preparation method. In *Proceedings First International Spring School and Symposium on Advances in Materials Science*, vol. 2, Cairo, Egypt, 1994, pp. 535-547.
12. Maschio, S. and Trovarelli, A., Powder preparation and sintering behaviour of ZrO_2–20 mol.–%CeO_2 solid solutions prepared by various methods. *Br. Ceram. Trans.*, 1995, **94**, 191–195.
13. Maschio, S., Bachiorrini, A. and Lucchini, E., Sintering behaviour of mechanically alloyed and coprecipitated 12Ce–PSZ powders. *J. Mater Sci.*, 1998, **33**, 3437–3441.
14. Muccillo, E. N. S. and Ávila, D. M., Synthesis and characterization of submicron zirconia-12 mol% ceria ceramics. *Cer. Int.*, 1999, **25**, 345–351.
15. Meriani, S., Thermal evolution of ceria–zirconia metallorganic precursors. *Thermochim. Acta*, 1982, **58**, 253–259.
16. Nagarajan, V. S. and Rao, K. J., Characterization of sol-gel derived zirconia with additions of yttria and ceria. Origin of high fracture toughness in ceria-stabilized samples. *Phil. Mag.*, 1992, **A65**, 771–781.
17. Torng, S., Miyazawa, K. and Sakuma, T., The diffusionless cubic-to-tetragonal phase transition in near-stoichiometric ZrO_2–CeO_2. *Cer. Int.*, 1996, **22**, 309–315.
18. Qiu, H., Gao, L., Feng, C., Guo, J. and Yan, D., Preparation and characterization of nanoscale Y-TZP powder by heterogeneous azeotropic distillation. *J. Mater Sci.*, 1995, **30**, 5508–5513.
19. Shan, H. and Zhang, Z., Preparation of nanometre-sized ZrO_2/Al_2O_3 powders by heterogeneous azeotropic distillation. *J. Eur. Ceram. Soc.*, 1997, **17**, 713–717.
20. Panova, T. I., Savchenko, E. P., Roshchina, E. V. and Glushkova, V. B., Comparative evaluation of methods of preparing partially stabilized zirconium dioxide. *J. Appl. Chem.*, 1990, **63**, 88–91.
21. Vogel, A. I., *Text Book of Macro and Semimicro Qualitative Inorganic Analysis*, 5th ed. Longman Group Ltd, London, UK, 1979.
22. Chiou, B. S., Lee, M. Y., Dai, H. T. and Duh, J. G., Thermal evolution and electrical properties of rare-earth oxide doped zirconia. In *Better Ceramics Through Chemistry III*, Mater. Res. Soc. 121, ed. C. J. Brinker, D. E. Clark, and D. R. Ulrich, 1988, pp. 605–610.
23. Sing, K. S., Everett, D. H., Haul, R. A. W., Moscou, L., Pierotti, R. A., Rouquerol, J. and Siemieniewska, T., Reporting physisorption data for gas/solid systems with special reference to the determination of surface area and porosity. *Pure Appl. Chem.*, 1985, **57**, 603–619.
24. Halloran, J. W., Role of powder agglomerates in ceramic processing. In *Advances in Ceramics, Forming of Ceramics 9*, ed. J. A. Mangels and G. L. Messing. Am. Ceram. Soc., Columbus, OH, 1984, pp. 67–75.
25. Kaliszewski, M. S. and Heuer, A. H., Alcohol interaction with zirconia powders. *J. Am. Ceram. Soc.*, 1990, **73**, 1504–1509.
26. Yashima, M., Ohtake, K., Kakihana, M., Arashi, H. and Yoshimura, M., Determination of cubic-tetragonal phase boundary in $Zr_{1-x}Y_xO_{2-x/2}$ solid solutions by Raman spectroscopy. *J. Appl. Phys.*, 1993, **74**, 7603–7605.